Biophysical Journal
Article

Biophysical Society

Optimal Background Estimators in Single-Molecule FRET Microscopy

Søren Preus,[1] Lasse L. Hildebrandt,[1] and Victoria Birkedal[1,2,*]
[1]Interdisciplinary Nanoscience Center and [2]Department of Chemistry, Aarhus University, Aarhus, Denmark

ABSTRACT Single-molecule total internal reflection fluorescence (TIRF) microscopy constitutes an umbrella of powerful tools that facilitate direct observation of the biophysical properties, population heterogeneities, and interactions of single biomolecules without the need for ensemble synchronization. Due to the low signal/noise ratio in single-molecule TIRF microscopy experiments, it is important to determine the local background intensity, especially when the fluorescence intensity of the molecule is used quantitatively. Here we compare and evaluate the performance of different aperture-based background estimators used particularly in single-molecule Förster resonance energy transfer. We introduce the general concept of multiaperture signatures and use this technique to demonstrate how the choice of background can affect the measured fluorescence signal considerably. A new, to our knowledge, and simple background estimator is proposed, called the local statistical percentile (LSP). We show that the LSP background estimator performs as well as current background estimators at low molecular densities and significantly better in regions of high molecular densities. The LSP background estimator is thus suited for single-particle TIRF microscopy of dense biological samples in which the intensity itself is an observable of the technique.

INTRODUCTION

Single-molecule total internal reflection fluorescence (TIRF) microscopy constitutes a powerful toolbox for studying the molecular biophysics and nanoscale interactions of biomolecules at the single-molecule level (1–3). In this technique a fluorescence microscope is used to record, track, and quantify the fluorescence signal of single isolated molecules, providing a means to observe molecular properties that are otherwise hidden behind an ensemble mean.

One technique that exploits the ability to measure fluorescence intensities of single isolated molecules is single-molecule Förster resonance energy transfer (smFRET), which can be implemented using TIRF microscopy (1,4–6). In smFRET, two fluorophores that are capable of exchanging excitation energy by FRET are attached to the biomolecules of interest. The measured fluorescence intensity ratio of the two dyes reflects the efficiency of energy transfer and is used as a measure of the interdye distance, which is typically on a 2–10 nm length scale. Since the obtained distance information represents the relative distance between the two labeling sites, this technique reports on the presence of both static and dynamic molecular states. Surface immobilization further allows molecules to be monitored during extended periods of time covering up to minutes and even hours. The resulting FRET time traces of each molecule can reveal information about molecular conformations, sample heterogeneity, and transitional state dynamics (7,8).

In many single-molecule fluorescence microscopy techniques, a correct measure of the local background intensity is of ultimate importance due to the low signal/noise ratio in such experiments (9). The measured molecule intensity signal is influenced by both fluctuations in camera shot noise (Poisson distributed) and photons coming from sources other than the molecule of interest, which is referred to as the background intensity (2). The background intensity can be affected considerably by a number of global and local effects, including inhomogeneous or fluctuating laser spot profiles and crowded molecular environments (10,11). Particularly in dense samples, photons coming from neighboring molecules may contribute substantially to the background intensity. This problem is demonstrated by comparing the FRET traces of the same molecule obtained using five different background estimators (Fig. 1, vide infra), four of which have been used in previous studies to estimate the fluorescence background intensity in smFRET TIRF microscopy.

Submitted October 14, 2015, and accepted for publication July 26, 2016.
*Correspondence: vicb@inano.au.dk
Editor: David Rueda.
http://dx.doi.org/10.1016/j.bpj.2016.07.047

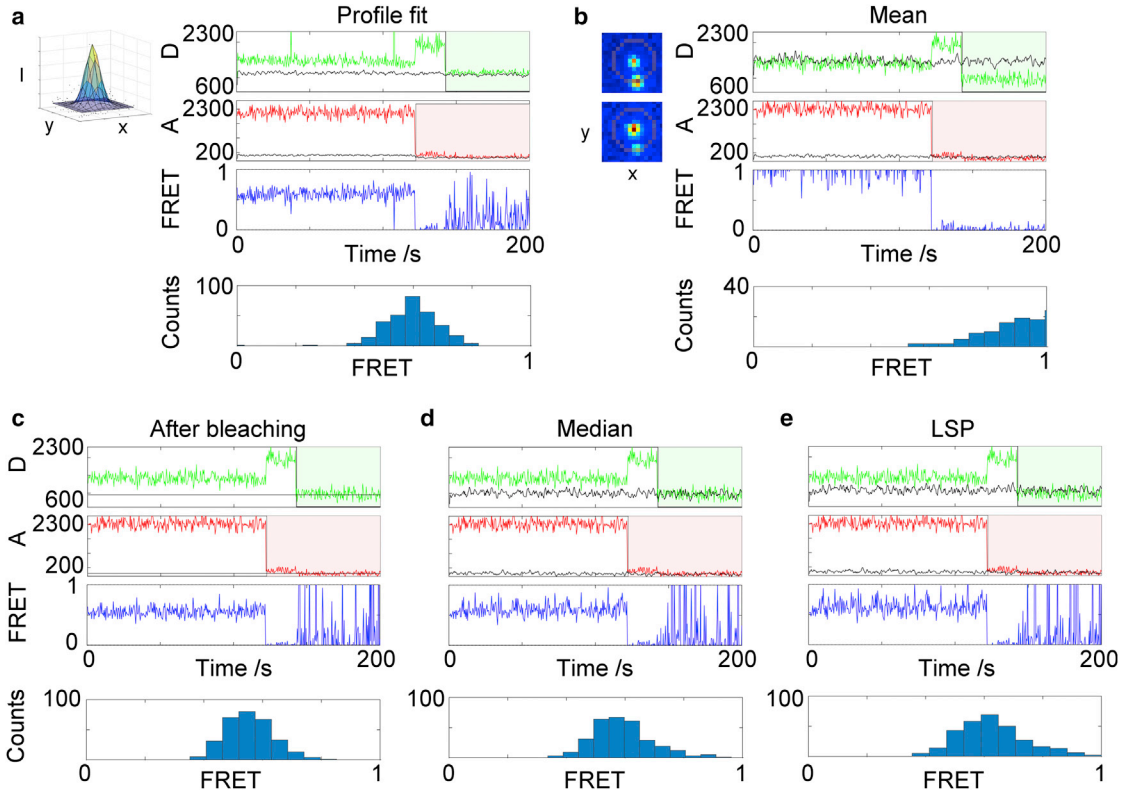

FIGURE 1 Five different background estimators applied to the same molecule (experimental data). (*a*) Gaussian profile fitting-based background estimator. The inset shows an example of the result of a profile fit. (*b–e*) Aperture-based background estimators. The background aperture (*highlighted ring* in the *upper-left inset* in (*b*) showing donor and acceptor fluorescence spots (*top and bottom images*, respectively)) overlaps a neighboring molecule in the donor channel. Traces shown are the raw background-uncorrected donor intensity (*green*), raw acceptor intensity (*red*), backgrounds (*black*), and FRET efficiencies (*blue*). The FRET histograms (*bottom*) only include frames until bleaching of the acceptor. The donor bleaches at 142 s and the acceptor bleaches at 122 s. Aperture-based background intensities were determined using (*b*) the local mean background, (*c*) the intensity after bleaching, (*d*) the local median background, and (*e*) the LSP background. To see this figure in color, go online.

Here, we evaluate the performance of traditional aperture-based background estimators used in smFRET TIRF microscopy. We show that in some cases, the choice of background estimator can have a critical influence on the observed fluorescence intensity. In particular, we demonstrate how a popular measure of the local background, the pixel distribution mean of a local background aperture surrounding the molecule of interest (5,12–15), is considerably perturbed at high molecular densities where photons coming from neighboring molecules contribute to the registered background pixel distribution. For working at high molecular densities, we propose a new, to our knowledge, simple background estimator that is based on the *X*th percentile of the local background aperture pixel distribution and thus is referred to as the local statistical percentile (LSP). The LSP background estimator is less affected by neighboring molecules compared with the local mean, and the LSP resembles the value of the mean when there are no neighbors of the molecule of interest. We show that the LSP background estimator performs as well as current background standards at low molecule surface densities and considerably better at high molecule densities.

MATERIALS AND METHODS

Single-molecule sample

PAGE-grade, purified, single-stranded DNA labeled with either a donor (Cy3) or an acceptor (Alexa Fluor 647) was purchased from IBA (Göttingen, Germany). The sequence of the donor-labeled strand was 5′-CGC GTC GGC AGC ATA CAA XAA CCT CAT CGA TAA GAA AGA AAT AAA GAA GAT CGC, where X marks an amino-modified dT labeled with Cy3 NHS. The 5′ end was labeled with a biotin, used for surface immobilization. The sequence of the acceptor strand was complementary to the donor strand: 5′-GCG ATC TTC TTT ATT TCT TTC YTA TCG ATG AGG TTA TTG TAT GCT GCC GAC GCG, where Y marks an amino-modified dT labeled with Alexa Fluor 647 NHS. Equimolar stoichiometries of donor and acceptor strands were annealed in TAE buffer (20 mM Tris/acetate/EDTA) at pH 8.3 and 100 mM KCl (Sigma-Aldrich, St. Louis, MO).

smFRET microscopy experiments

smFRET experiments were performed using alternating laser excitation as described previously (6,16). DNA molecules were immobilized via biotin-streptavidin linkage on a quartz coverglass for prism TIRF microscopy. Fluorescence was measured using an inverted wide-field optical microscope and alternate laser excitation at 514 and 630 nm of the donor and acceptor fluorophore, respectively. Fluorescence movies of several minutes were

recorded with an electron-multiplying charge-coupled device (EMCCD) camera (iXon3 897; Andor, Belfast, Northern Ireland) with a 200 ms integration time per image.

The imaging buffer used in the smFRET experiment was the same as the annealing buffer but contained in addition an enzymatic oxygen scavenging system consisting of glucose oxidase (16.67 units/mL; Sigma-Aldrich), catalase (260 units/mL; Sigma-Aldrich), B-D-(+)glucose (4.5 mg/mL; Sigma-Aldrich), and (±)-6-hydroxy-2,5,7,8-tetramethylchromane-2-carboxylic acid (2 mM, Trolox; Sigma-Aldrich). Halfway through the acquisition, the imaging buffer was substituted to the annealing buffer to facilitate bleaching.

Data analysis was performed using the smFRET microscopy software package iSMS (http://isms.au.dk) (17). Colocalized donor/acceptor fluorescence spots were identified. Donor and acceptor intensities of individual molecules were calculated via aperture photometry using an aperture centered on the pixel in the spot showing highest intensity, with a width of 5 pixels and a ring background of 1 pixel width located at a radius of 2 pixels outside the edge of the molecule aperture. The fluorescence intensities depended on the size of the chosen aperture, which did not significantly affect the experimentally determined FRET signal, as FRET is a ratiometric method. Increasing the size of the background ring decreased the noise level of the background signal but had a negligible effect on FRET histograms in our conditions. Relative FRET efficiencies were obtained from the donor and acceptor fluorescence intensities after background corrections as

$$E = \frac{I_{FRET}}{I_{FRET} + \gamma \times I_D^D}. \quad (1)$$

Here I_D^D and I_{FRET} denote the fluorescence intensities observed in the donor and acceptor emission channels, respectively, after donor excitation. The latter is corrected for direct excitation of the acceptor at the donor excitation wavelength and leakage of donor emission into the red emission channel using the approach described by Lee et al. (18) and Margeat et al. (19). The factor γ corrects for differences in brightness and detection efficiency between the donor and acceptor fluorophores. smFRET histograms contain only data from dual-labeled molecules before fluorophore bleaching. The correction factors were $A_{\text{direct}} = 0.06$, $D_{\text{leakage}} = 0.11$, and $\gamma = 2.5$.

Background estimators

The background-corrected fluorescence intensity of the molecule, I_{molecule}, was calculated at each frame as $I_{molecule} = I_{raw} - I_{back}$. Here, I_{raw} is the total photon count and I_{back} is the background intensity. I_{raw} was determined by aperture photometry using a disk-shaped aperture (mask) of radius r centered at the peak coordinates of the molecule, as $I_{raw} = \sum_{i=1}^{n_{\text{pixels}}} I_i$, which is the sum of the photon counts of all n_{pixels} within the integration mask. Five different methods were used to determine I_{back}:

1) The local background mean estimator (5,12–15,20) was calculated as the mean value of the pixel distribution within a local background aperture:

$$I_{back}^{avg} = n_{pixels} * \text{avg}(I_{back,mask}), \quad (2)$$

where $\text{avg}(I_{\text{back,mask}})$ is the average photon count in a local square or ring-shaped background aperture surrounding the molecule.

2) The intensity after bleaching background estimator (1,5) was calculated as the mean intensity of the molecule in a time-interval after the molecule has bleached:

$$I_{back}^{bleach} = \frac{\sum_{i=t_1}^{t_2} I_i}{t_2 - t_1}, \quad (3)$$

where t_1 and t_2 are two time points after the molecule has bleached.

3) The local median estimator was calculated as the median value of the pixel distribution within the local background aperture (1,21):

$$I_{back}^{med} = n_{pixels} * \text{median}(I_{back,mask}). \quad (4)$$

The background aperture was the same as that used for the local mean background estimator.

4) The LSP was calculated as the Xth percentile of the pixel distribution of the local background aperture:

$$I_{back}^{LSP} = n_{pixels} * \text{LSP}(I_{back,mask}). \quad (5)$$

The Xth percentile ($0 < X < 100$) of a distribution is the smallest value in the ordered list of distribution values (sorted from least to greatest) such that X% of the pixels is less than or equal to that value. When X equals 50%, the LSP is identical to the median.

5) The background-corrected fluorescence intensity of the molecule was obtained as (15)

$$I_{molecule} = 2\pi * s_x * s_y * A \quad (6)$$

by fitting a two-dimensional (2D) Gaussian function to a small pixel window of the molecule of interest at each frame. The Gaussian function was given by

$$I(x,y) = A * \exp\left[-\left(\frac{x'^2}{2s_x^2} + \frac{y'^2}{2s_y^2} \right) \right] + B, \quad (7)$$

where A is the amplitude, B is the background, s_x and s_y are the Gaussian widths (standard deviation), and x' and y' are given by $x' = (x - x_0) * \cos(\theta) - (y - y_0) * \sin(\theta)$ and $y' = (x - x_0) * \sin(\theta) + (y - y_0) * \cos(\theta)$. Here, x_0 and y_0 are the center coordinates, and θ is the angle of rotation.

The optimization was performed using least-squares fitting, and no fit parameters were constrained.

Software toolkit with background estimators in smFRET

All of the background estimators evaluated here, as well as the method of multiaperture signatures (vide infra), are provided as new toolkits for the smFRET microscopy software iSMS (see www.isms.au.dk/download). A protocol for determining the value of X in the LSP model using iSMS is provided in the documentation of the software at www.isms.au.dk.

Simulations

Simulations of synthetic samples with increasing molecule surface density were performed using MATLAB R2014b (The MathWorks, Natick, MA). The (x,y) pixel positions of simulated molecules were randomized using only the total molecule coverage surface density as the constraint. Pixels representing molecules were set to an initial value of 500 and subjected to 2D Gaussian filtering. The resulting molecule point spread function (PSF) width was 1.2 pixels with an integration aperture width of 5 pixels. A Gaussian noise profile with a mean level of 10 and a variance of 3 was added. The simulations shown are the result of 5000 molecules, with a total movie length of 20 frames. The shown background distributions are the binned histogram of all background frames of all molecules in the simulation. The true background distribution was simulated by running the same simulation on a theoretical sample in which all molecules were aligned in a grid so that each peak did not overlap the background aperture of its neighbors. The background aperture was a ring-shaped mask surrounding the

molecule at a radius of 2 pixels outside the molecule intensity mask, corresponding to a radius of 5 pixels from the molecule center.

RESULTS AND DISCUSSION

Performance of traditional background estimators

The choice of background estimator affects the value of the background-corrected fluorescence intensity of a molecule (Fig. 1). In many single-molecule techniques, the background-corrected intensity is obtained by fitting a mathematical model function to the PSF of the molecule intensity peak, referred to as profile fitting (see (22) and references therein). Usually a 2D Gaussian PSF is assumed, in which case the background-corrected intensity of the molecule is determined directly from the fitted model parameters (see Fig. 1 *a* and Materials and Methods section). Another advantage of using profile fitting is that the Gaussian model parameters may contain insightful information about the peak of interest, such the number of molecules within the spot (15), the subpixel localization of the molecule (22,23), or the distance from the fluorophore to the surface of the sample (24). The disadvantage of the PSF estimator is that it relies heavily on the goodness of the fit, which in turn relies on start guesses and constraints on model parameters, the signal/noise ratio of the data, and the presence of molecules close to the molecule of interest. Profile fitting additionally relies on choosing a proper region of interest around the molecule to fit (22); the actual PSF of the molecule is not necessarily Gaussian distributed, but is a function of the optical setup and fluorophore environment (22,23,25).

Aperture-based fluorescence intensities and background estimators are used, alongside Gaussian profile fitting, in smFRET TIRF microscopy. A common background estimator is the mean pixel intensity within a local background aperture surrounding the molecule of interest (Fig. 1 *b*, *inset*) (5,12–15,20). The advantage of the local aperture mean is that it is simple, fast, and robust when the peak of interest in the image frame is well isolated from neighboring peaks (17). In this work, the use of background estimators based on local apertures was much faster computationally (by orders of magnitude) than Gaussian profile fitting. The disadvantage of the local aperture mean is that it is severely perturbed by the presence of neighboring molecules and transient background signals in the vicinity of the fluorescence peak (Fig. 1 *b*). This property is due to the intrinsic dependency of the mean value on statistical outliers (i.e., photons coming from the neighboring molecule). Thus, an incorrectly high background is registered for molecules in which the local background aperture includes photons coming from neighboring molecules.

A second popular background estimator that circumvents the problem of the aperture mean is the intensity that remains after the molecule has bleached (Fig. 1 *c*) (1,5). This background estimator is calculated as the mean intensity within the molecule aperture within a time interval after bleaching. The advantage of using the intensity after bleaching is that this value is unperturbed by neighboring molecules and provides the correct background intensity when there are no time fluctuations of the background signal. The disadvantage of this estimator is the requirement of bleaching within the observable time window and the inability of this estimator to account for background signals fluctuating in time.

A third, less widely used estimator of background in single-molecule TIRF microscopy is the pixel median value of a local background aperture of the peak (14). The aperture chosen is either a large pixel window that includes the peak itself (21) or, as in this work, a ring-shaped aperture surrounding the molecule of interest. The advantage of the median statistic is that it is inherently less affected by pixel outliers and extremes, such as large pixel values resulting from emitting neighboring molecules, compared with the distribution mean. For this reason, the median estimator may capture the value of the background even when there are one or more molecules surrounding the molecule of interest and included in the background aperture (Fig. 1 *d*).

The local median background estimator scales better with molecule surface density

The advantage of a percentile-based background estimator, such as the median, over a local mean estimator is demonstrated in Fig. 2. Here, we simulated noisy microscopy movies of a population of immobilized molecules. The background intensity distribution of all the frames of all the randomly distributed molecules in the movie was calculated using a local background aperture mean and compared with the same distribution obtained using a median-based background aperture (Fig. 2 *a*). We compared the two background estimators by varying only the molecule surface density and keeping the background noise and molecule intensities constant. We then compared the background intensity pixel distributions obtained with each of the two background estimators against the true background intensity distribution. The true background distribution was calculated using the same background estimator applied on a simulated reference sample in which all molecules were aligned in an ordered point array (Fig. 2 *b*). For simplicity, the background noise was assumed to be normally distributed in the simulations. As a result of this assumption, the mean and median-based background estimators return the same value when the molecules are well separated from each other (Fig. 2 *a*, *upper panel*). This feature is not observed in experiments in which the mean and median background estimators do not have the same value (vide infra). However, in conditions of low molecular surface coverage, the differences between the mean and median values are relatively small both experimentally and in test simulations using non-normal distributions. Thus, our

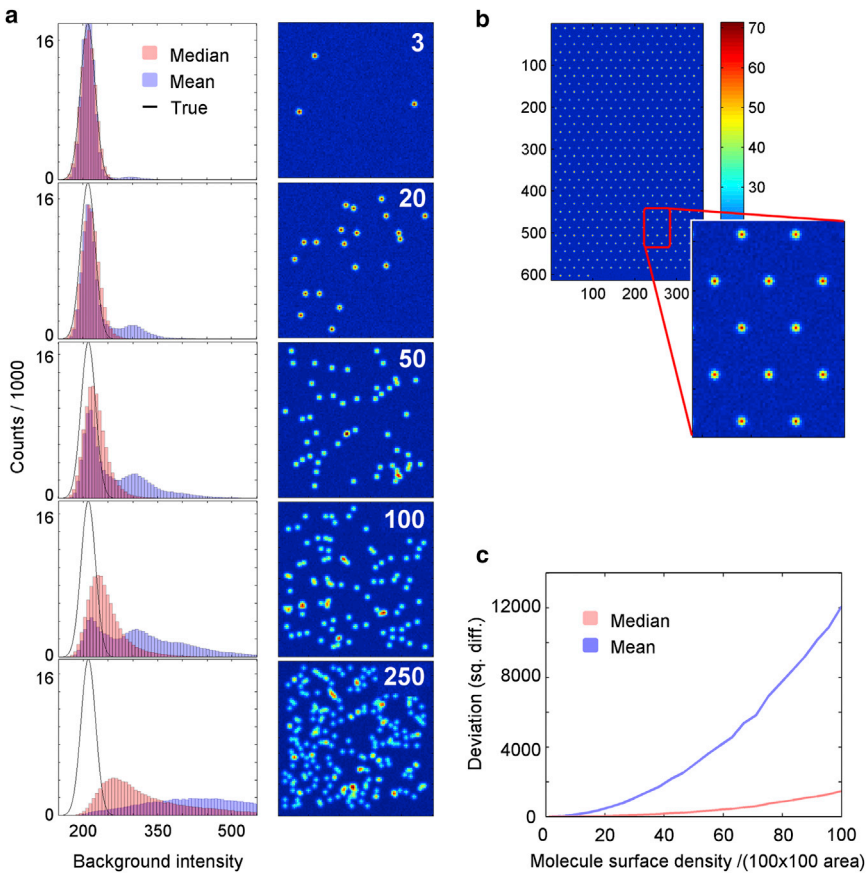

FIGURE 2 Simulations of background distributions at increasing molecular surface densities (simulated data). (*a*) Background pixel distributions (*left*) determined using the local mean (*blue*) and local median (*red*) background estimators, compared with the true distribution (*black*). The images show the corresponding molecular surface density, with the density shown in the inset in units of molecules/(100 × 100 pixels). (*b*) Calculation of the true background distribution using a reference array in which neighboring molecules do not interact. (*c*) Comparison of the squared difference between the mean of the determined and true background distributions as a function of surface density. To see this figure in color, go online.

simulations show that mean and median background estimators are influenced differently by the molecule surface density and coverage.

The advantage of the median-based estimator over the mean estimator can be seen by comparing the deviation of the measured background distributions with the true distribution at increasing molecule surface density (Fig. 2 *c*). The overall increased deviation at increasing molecule density results from the fact that the local background aperture of each molecule is perturbed by photons accumulated from neighboring molecules. As shown in the figure, the background determined using a median-based local aperture scales considerably better than the mean background estimator. In fact, the same background accuracy was achieved at 3–4 times higher surface density when the median estimator was used compared with the mean estimator. This is because the median estimator is less affected by extreme values in the pixel distribution of the background aperture corresponding to neighboring molecules.

The local median estimator underestimates the residual background intensity

As shown above, the local aperture median background estimator performs considerably better than the mean background estimator when other molecules contribute to the background pixel distribution in the vicinity of the molecule of interest (Figs. 1 and 2). The disadvantage of the median estimator, however, is that the median pixel distribution value underestimates the background intensity in regions with little to no fluorescence signal (Fig. 3 *a*). This problem arises because the pixel value distribution of the background aperture in empty regions in the image is not symmetrically distributed around the mean, but rather is characterized by a positive skew resulting from the EM gain of the EMCCD camera combined with Poissonian shot noise (Fig. 3 *b*) (26–28). The distribution skew is a property of the residual background and thus also contributes to the raw fluorescence intensity sum of the pixels in the molecule aperture. However, the skew is not adequately taken into account by the median background estimator, resulting in a background-corrected fluorescence signal that is larger than zero in regions where the fluorescence intensity is in fact zero.

Although the disadvantage of the median estimator discussed above usually has a small effect on molecule fluorescence intensity, the underestimated background intensity can be important in smFRET experiments where the intensity that remains after acceptor bleaching is used to calculate correction factors for cross talk between the donor and acceptor channels (6,18,19).

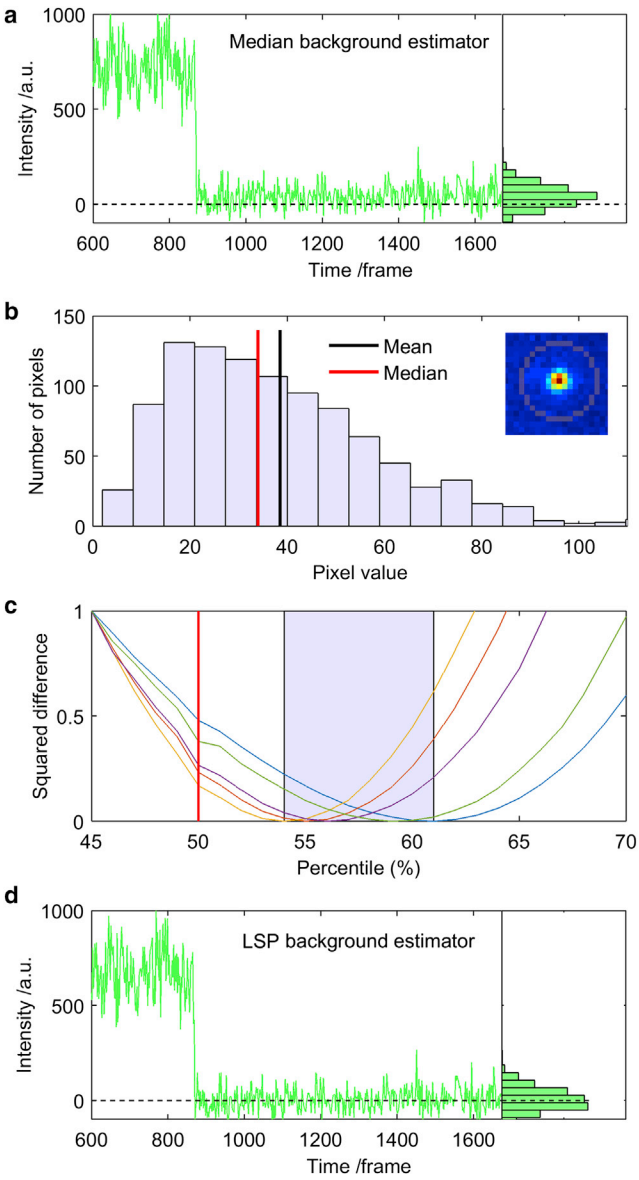

FIGURE 3 Percentile-based background estimators (experimental data). (*a*) Background-corrected intensity trace using a median-based background estimator. Although the molecule bleaches at frame 870, the background-corrected intensity does not decay to zero, as shown by the binned histogram. The histogram includes frames after bleaching only. (*b*) Background pixel distribution of a blank region (*inset*), showing why the background-corrected intensity in figure (*a*) does not decay to zero. The background pixel distribution is characterized by a positive skew resulting in a lower distribution median value (*red*) compared with the distribution mean (*black*). As a result, the median background estimator underestimates the background intensity. The histogram bins pixels from 100 frames from the background aperture. (*c*) Squared difference (normalized at 45%) between the background pixel distribution mean and percentile for five experimental conditions differing in laser intensity and EM gain. The optimal percentile yields the value that resembles the mean and is generally between 54% and 61% (highlighted interval). The red vertical line denotes the percentile corresponding to the median value (50%). (*d*) Background-corrected intensity trace of the same molecule as in (*a*) but with a percentile-based background estimator ($X = 56\%$). Here, the intensity decays to zero after bleaching. To see this figure in color, go online.

LSP background estimator

To address the problems of each of the background estimators described above, we propose a fourth background estimator, referred to as the LSP. The LSP background estimator is calculated as the Xth percentile of the pixel distribution of the local background aperture. The optimal value of X is determined as the background pixel distribution percentile that is closest to the mean value of the distribution for an empty pixel window, i.e., a mask containing little to no fluorescence signal from molecules. The mask used for the blank distribution could be, e.g., the local background aperture of an isolated molecule. The value of X is also the value that produces an average background-corrected fluorescence signal of zero after a molecule has bleached. The value of X only needs to be calculated for a few molecules in a given experimental setup. In our tested setups, the optimal value of X was generally in a narrow range of 54–61% (Fig. 3 *c*).

Our motivation for introducing the LSP is that similarly to the median estimator, this statistic is less affected by population extremes (i.e., photons accumulated from neighboring molecules) compared with the mean of the distribution. However, as opposed to the median background estimator, the LSP is designed to resemble the mean value of the background pixel distribution when there are no molecules, thus producing a background-corrected fluorescence signal of zero when there are no emitting molecules (Fig. 3 *d*). It is noted that for $X = 50\%$, the LSP is identical to the median estimator, whereas with increasing values of X the LSP becomes less resilient to the presence of neighboring molecules compared with the median.

Multiaperture signatures and performance of background estimators in common situations

The performance of different background estimators depends on the chosen aperture size. To avoid any effects from this parameter, we compared the performance and properties of the mean, median, and LSP background estimators by using multiaperture signatures of molecules typically encountered in smFRET (Fig. 4). We calculated these multiaperture signatures by systematically varying the aperture size of the molecule and observing the concomitant change in the determined background-corrected intensity and associated background. Here, the aperture size was defined as the width of the inner molecule aperture disk while the background aperture ring was located 1–2 pixels outside the molecule aperture (Fig. 4 *a*). When the size of the aperture increases, the background-corrected intensity increases simply because more photons are included in the aperture (Fig. 4 *b*, *middle*). At the same time, the background decreases because fewer photons coming from

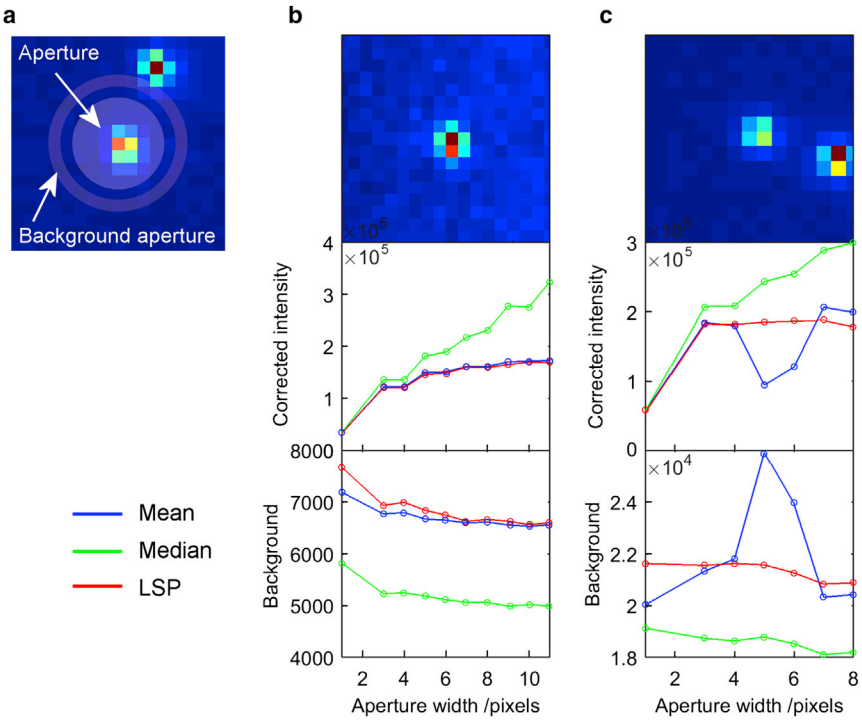

FIGURE 4 Comparison of the performance of the local mean, median, and LSP background estimators in different molecular environments (experimental data). (*a*) Schematic representation of the molecule aperture and the background aperture surrounding the molecule. The aperture width is the width of the inner aperture. (*b* and *c*) Multiaperture signatures of representative molecules with varying local density. The corrected intensity is the background-subtracted donor intensity until the time of bleaching as a function of the molecule aperture size. The background is the total donor background intensity until the time of bleaching. (*b*) Single isolated molecule. (*c*) Molecule in regions where a neighbor is located within a distance of 5–10 pixels from the molecule of interest. In both cases, the aperture is centered on the highest-intensity pixel in the spot of the molecule under consideration. To see this figure in color, go online.

the molecule are included in the background aperture (Fig. 4, *b* and *c*, *bottom*).

For single isolated molecules, the background-corrected intensity should reach a plateau when the aperture size increases, i.e., when all photons coming from the molecule are included in the aperture. This plateau is observed for the intensity determined using the mean and LSP background estimators (Fig. 4 *b*, *blue* and *red*). The intensity calculated using the median background estimator, on the other hand, does not reach a plateau (Fig. 4 *b*, *green*). This observation is a direct result of the median background estimator underestimating the residual background as discussed above.

In situations where photons coming from neighboring molecules are included in the background aperture, the median and LSP background estimators perform considerably better than the mean estimators (Fig. 4 *c*). The presence of neighboring molecules is observed as a spike as the background aperture overlaps the neighboring molecule (Fig. 4 *c*, *blue*). The intensity determined using the mean background estimator is considerably perturbed when the aperture size is located at the spike (Fig. 1 *b*). This spike is not seen in either the median or the LSP background estimators, both of which exclude the high-intensity pixel extremes in the background pixel distribution (Fig. 4 *c*, *green* and *red*).

It is noted that the method of multiaperture signatures provides a general, in-depth characterization of individual spots observed in single-molecule TIRF microscopy. In particular, the characteristic features of multiaperture signatures suggest that multiaperture signatures can be used for quality control and automated sorting of smFRET data.

Dependency of the smFRET histogram on the choice of background estimator

Although the background estimators performed almost equally well in sparse regions, the choice of background estimator was important in dense sample regions. To illustrate this, we compare the smFRET distributions of a population of DNA molecules using the five different background estimators, including both profile fitting and aperture-based photometry (Fig. 5). To facilitate a proper comparison of the background estimators, all of the shown histograms were calculated on the same set of samples but in regions of different surface density. In regions of low surface density, where molecules are separated by a distance larger than the radius of the background aperture, the resulting FRET distributions obtained using the five different background estimators display a similar appearance (Fig. 5, *a*, *left*, and *b*, *open circles*). In regions of high molecule surface density, where photons from neighboring molecules contribute to the counts registered by the background aperture, the smFRET distributions are clearly influenced by the choice of background estimator in both the peak FRET efficiency and the width of the distribution (Fig. 5 *a*). The smFRET distributions of molecules located in sparse and dense regions differ considerably more when the mean background estimator is used compared with the other estimators (Fig. 5 *a*, *right*, and *b*, *closed circles*).

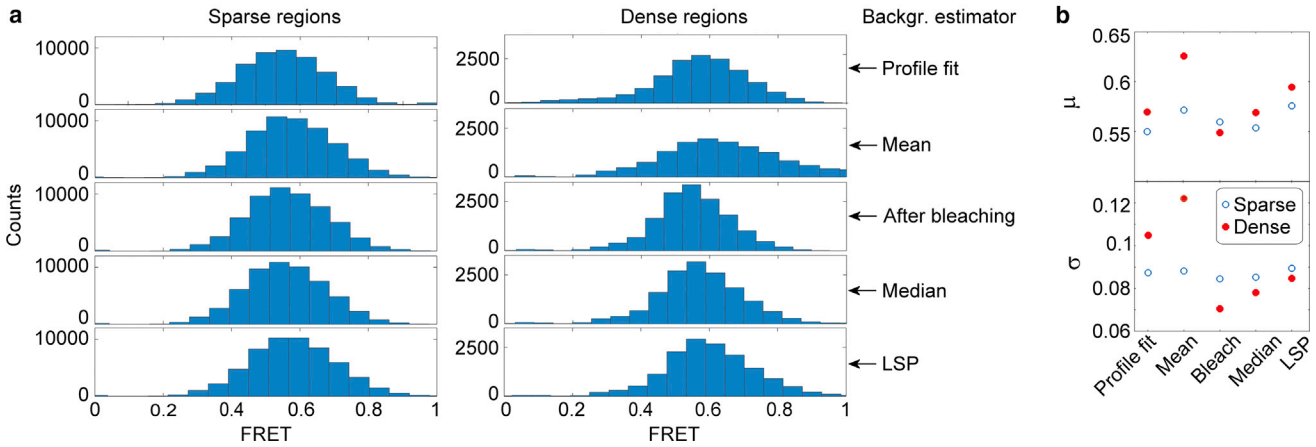

FIGURE 5 Effect of background on smFRET histograms. (*a*) Comparison of FRET histograms of the same sample in regions of varying density, determined using five different background estimators (experimental data). The histogram of the sparse molecular regions (*left*) contains 229 double-stranded DNA molecules. The histogram of dense molecular regions (*right*) contains 65 molecules. Dense regions are defined as molecular regions in which neighbors contribute photons to the background aperture (7–8 pixels; see Fig. 2, *d* and *f*), whereas sparse regions consist of isolated molecules (see Fig. 2, *b* and *c*). The FRET histograms contain only molecules in which both the donor and acceptor bleach in one step, and only frames obtained before the first bleaching event. (*b*) E_{mean} (μ) and $E_{\text{std.dev.}}$ (σ) obtained from a normal distribution fit of each of the histograms in (*a*). To see this figure in color, go online.

The smFRET distribution determined using the local mean background estimator is generally broader in denser regions and is centered at a higher FRET efficiency compared with the histogram for molecules in sparse regions, as shown by the normal distribution fits (Fig. 5 *b*). The intensity-after-bleaching estimator generates the narrowest FRET distribution as a result of this estimator corresponding to a constant background throughout the time trace of each molecule.

CONCLUSIONS

We have compared and evaluated different estimators of the background intensity in single-molecule TIRF microscopy. If the background does not change over time and the molecule bleaches within the observation time window, the intensity that remains after molecule bleaching is a robust measure of the background. In situations where it is not possible to apply this estimator (e.g., tracking experiments (29), backgrounds that fluctuate in time, and molecules that do not bleach), we suggest that an optimal percentile of the pixel distribution of a local background aperture of the intensity peak is a simple, fast, and robust alternative to current background standards. At low molecule densities, this LSP estimator performs as well as current estimators, and it performs considerably better in dense regions of molecules.

In this work, multiaperture signatures were introduced as a general tool and provided insight into the performance of different background estimators in common situations found in smFRET. We compared the effects of different background estimators in smFRET TIRF microscopy and found that the choice of background influenced the measured FRET efficiency for molecules located in regions of high molecule surface density.

AUTHOR CONTRIBUTIONS

S.P. and V.B. designed the research and wrote the manuscript. L.L.H. performed experiments. S.P. wrote the software. S.P., L.L.H., and V.B. analyzed data.

ACKNOWLEDGMENTS

We thank Daniel Gudnason for technical assistance.

This work was supported by the Danish Council for Independent Research through a Sapere Aude II grant (DFF-0602-01670), by the Danish National Research Foundation to center of DNA nanotechnology (DNRF 81), and by the Aarhus University Research Foundation.

REFERENCES

1. Ha, T., T. Enderle, …, S. Weiss. 1996. Probing the interaction between two single molecules: fluorescence resonance energy transfer between a single donor and a single acceptor. *Proc. Natl. Acad. Sci. USA.* 93:6264–6268.
2. Moerner, W. E., and D. P. Fromm. 2003. Methods of single-molecule fluorescence spectroscopy and microscopy. *Rev. Sci. Instrum.* 74: 3597–3619.
3. Joo, C., H. Balci, …, T. Ha. 2008. Advances in single-molecule fluorescence methods for molecular biology. *Annu. Rev. Biochem.* 77:51–76.
4. Joo, C., and T. Ha. 2012. Single-molecule FRET with total internal reflection microscopy. *Cold Spring Harb. Protoc.*, pii: pdb.top072058.
5. Roy, R., S. Hohng, and T. Ha. 2008. A practical guide to single-molecule FRET. *Nat. Methods.* 5:507–516.
6. Krüger, A. C., and V. Birkedal. 2013. Single molecule FRET data analysis procedures for FRET efficiency determination: probing the conformations of nucleic acid structures. *Methods.* 64:36–42.
7. Hildebrandt, L. L., S. Preus, …, V. Birkedal. 2014. Single molecule FRET analysis of the 11 discrete steps of a DNA actuator. *J. Am. Chem. Soc.* 136:8957–8962.
8. Hohlbein, J., T. D. Craggs, and T. Cordes. 2014. Alternating-laser excitation: single-molecule FRET and beyond. *Chem. Soc. Rev.* 43:1156–1171.

9. Hoogendoorn, E., K. C. Crosby, …, M. Postma. 2014. The fidelity of stochastic single-molecule super-resolution reconstructions critically depends upon robust background estimation. *Sci. Rep.* 4:3854.
10. Betzig, E., G. H. Patterson, …, H. F. Hess. 2006. Imaging intracellular fluorescent proteins at nanometer resolution. *Science.* 313:1642–1645.
11. Hess, S. T., T. J. Gould, …, M. D. Mason. 2009. Ultrahigh resolution imaging of biomolecules by fluorescence photoactivation localization microscopy. *Methods Mol. Biol.* 544:483–522.
12. Solomatin, S. V., M. Greenfeld, …, D. Herschlag. 2010. Multiple native states reveal persistent ruggedness of an RNA folding landscape. *Nature.* 463:681–684.
13. Schluesche, P., G. Stelzer, …, M. Meisterernst. 2007. NC2 mobilizes TBP on core promoter TATA boxes. *Nat. Struct. Mol. Biol.* 14:1196–1201.
14. Howell, S. B. 1989. Two-dimensional aperture photometry signal to noise ratio of point source observations and optimal data extraction techniques. *Publ. Astron. Soc. Pac.* 101:616–622.
15. Holden, S. J., S. Uphoff, …, A. N. Kapanidis. 2010. Defining the limits of single-molecule FRET resolution in TIRF microscopy. *Biophys. J.* 99:3102–3111.
16. Krüger, A. C., L. L. Hildebrandt, …, V. Birkedal. 2013. Structural dynamics of nucleic acids by single-molecule FRET. *Methods Cell Biol.* 113:1–37.
17. Preus, S., S. L. Noer, …, V. Birkedal. 2015. iSMS: single-molecule FRET microscopy software. *Nat. Methods.* 12:593–594.
18. Lee, N. K., A. N. Kapanidis, …, S. Weiss. 2005. Accurate FRET measurements within single diffusing biomolecules using alternating-laser excitation. *Biophys. J.* 88:2939–2953.
19. Margeat, E., A. N. Kapanidis, …, S. Weiss. 2006. Direct observation of abortive initiation and promoter escape within single immobilized transcription complexes. *Biophys. J.* 90:1419–1431.
20. Greenfeld, M., D. S. Pavlichin, …, D. Herschlag. 2012. Single molecule analysis research tool (SMART): an integrated approach for analyzing single molecule data. *PLoS One.* 7:e30024.
21. McCann, J. J., U. B. Choi, …, M. E. Bowen. 2010. Optimizing methods to recover absolute FRET efficiency from immobilized single molecules. *Biophys. J.* 99:961–970.
22. Small, A., and S. Stahlheber. 2014. Fluorophore localization algorithms for super-resolution microscopy. *Nat. Methods.* 11:267–279.
23. Deschout, H., F. Cella Zanacchi, …, K. Braeckmans. 2014. Precisely and accurately localizing single emitters in fluorescence microscopy. *Nat. Methods.* 11:253–266.
24. Pinkney, J. N. M., P. Zawadzki, …, A. N. Kapanidis. 2012. Capturing reaction paths and intermediates in Cre-loxP recombination using single-molecule fluorescence. *Proc. Natl. Acad. Sci. USA.* 109:20871–20876.
25. Mortensen, K. I., L. S. Churchman, …, H. Flyvbjerg. 2010. Optimized localization analysis for single-molecule tracking and super-resolution microscopy. *Nat. Methods.* 7:377–381.
26. Chao, J., S. Ram, …, R. J. Ober. 2013. Ultrahigh accuracy imaging modality for super-localization microscopy. *Nat. Methods.* 10:335–338.
27. Chao, J., E. S. Ward, and R. J. Ober. 2012. Fisher information matrix for branching processes with application to electron-multiplying charge-coupled devices. *Multidimens. Syst. Signal Process.* 23:349–379.
28. Robbins, M. S., and B. J. Hadwen. 2003. The noise performance of electron multiplying charge-coupled devices. *IEEE Trans. Electron Devices.* 50:1227–1232.
29. Tyagi, S., V. VanDelinder, …, E. A. Lemke. 2014. Continuous throughput and long-term observation of single-molecule FRET without immobilization. *Nat. Methods.* 11:297–300.